Time-correlated Luminescence Blinking in InGaN Single Quantum Wells

Shunra Yoshida[1], Yusuke Fujii[1], Giovanni Alfieri[2], Ruggero Micheletto[1*1]

1. Yokohama City University, 22-2 Seto, Kanazawa-ku, 236-0027, Japan

2. Hitachi Energy, Fabrikstrasse 3, 5600 Lenzburg, Switzerland

(*Electronic mail: ruggero@yokohama-cu.ac.jp)

(Dated: 6 April 2023)

The blinking phenomenon in InGaN single quantum wells is a phenomenon where localized photoluminescence changes over time. Understanding its physics is important for the manufacture of more efficient light emission diodes. We present a study using two InGaN single quantum well samples, emitting at 460 nm and 510 nm wavelength, respectively. We confirmed that the luminescence intensity fluctuates in localized blinking regions and we found that these optical variations are not random, but are instead correlated in pairs, with either positive or negative coefficient, to a distant reference blinking point. Measurements were performed to obtain standard deviation and cross correlation maps. Invoking the quantum confined Stark effect we realized a simple phenomenological model that shows how charge carriers are exchanged among pairs of adjacent opposite correlation regions. As a result, it is suggested that the phenomenon is caused by fluctuations in the number of these exchanged carriers. Our model gives an explanation for the blinking phenomenon in InGaN single quantum wells and it is important for a deeper understanding to InGaN-based materials.

Understanding the fundamental properties and carrier dynamics of GaN and InGaN is essential for the development of GaN-based light emitting diodes (LED) devices and other applications. However, this is challenging due to the effects of a high defect density, the influence of large strain-induced polarization (caused by lattice mismatch) and also the lack of a suitable theoretical background[1,2]. The optical blinking phenomenon (BP) affecting the local luminescence in InGaN single quantum wells (QW) is one of these unknown phenomena that needs to be clarified.
The BP in InGaN QW was firstly observed by Micheletto et al.[3] with photo luminescence (PL) measurements. The phenomenon is triggered by illumination with light at 365 nm exciting both InGaN and GaN layer and occurs in a region of stronger optical emission compared to the average (intense luminous centers, ILCs). As most ILC's show stable optical emission, presence of blinking regions indicates locally high In composition and variable accumulation of carriers[4–7]. For this reason, the relationship between blinking and spatial inhomogeneity of In composition was discussed[8]. Depending on the indium concentration the BP phenomenon changes. For example, samples emitting 460 nm light optical blinking is observed, but less prominent and noticeable than for samples emitting green light such as those emitting at 510 nm and 540 nm[3,4].

Optical instabilities, such as blinking, are also reported in other materials like CdSe nanocrystals[9] and GaAs quantum dots (QD)[10]. Although these instabilities can be treated as an on/off flashing and explained with Auger ionization as in CdSe nanocrystals[9], this explanation cannot be applied to our InGaN quantum well samples where the blinking has not a simple on/off behaviour[11,12]. A comparison study of our sample blinking and blinking due to quantum jump model has been done in previous studies[3].

Several theories exist that could explain BP. One of them is quantum confined Stark effect (QCSE)[3,13,14], where the electric field changes the overlap of the electron and hole wavefunctions inside a quantum well. It is known that the piezoelectric field present in strained quantum wells composed of GaN and InGaN causes QCSE[15]. In addition, QCSE was also used to qualitatively explain the optical memory effect in InGaN thin film[16]. Since in this model the emission wavelength shortens with increasing intensity, it can explain the tiny shift in emission wavelength in BP, i.e. the wavelength becomes shorter when the intensity increases, and vice versa, due to the electric field of carriers trapped in deep levels[3,14]. These deep levels are possibly originating from defects at the InGaN/GaN interface[17,18]. However, the QCSE model cannot explain other experimental results such as intensity distribution and dynamics for the BP[3,19]. In another candidate model, interference of thermal vibration of the crystal lattice is implied as the cause of instability

in InGaN single QW[19], but it can not sufficiently explain other experimental features of blinking.

In a recent study, it was found that the adsorption of gas at different pressures, such as oxygen to the surface of the InGaN QW, increases the presence of ILCs and BP[20]. A similar effect was confirmed[21] by PL observation of the samples immersed in liquids. It was suggested that blinking could be caused by the interaction of surface molecules with impurities present within the QW. Based on such recent results and in order to obtain a more detailed insight between the BP and the role of defects. In this study, we report on the spatial time-correlation between blinking points in InGaN single QW and give a qualitative explanation of the BP based on our PL results.
In this study, the InGaN single QW samples are stacked over a 4 μm undoped GaN layer, a 3 nm $In_xGaN_{(1-x)}$ active layer, a 5 nm undoped GaN capping layer and they were grown along the (0001) direction by metal-organic vapor phase epitaxy (MOVPE) on sapphire. The emission peaks of the samples depend on the In concentration x in the Indium layer. The peak can range between 400 nm up to 540 nm or more[5]. In this study we used two samples that emit at 460 nm and 510 nm wavelength.

Samples were cleaned by one minute ultrasound sonic bath (US-2R, AS ONE, Japan) in distilled water before PL measurements. The measurements recorded with a CCD camera (HDR-SR1, SONY) attached to a selective excitation fluorescence microscope (BX51WX, Olympus). The optical emission from the surface was recorded at 30 frames per seconds and stored in a 730x730 pixels AVI format. Our recordings were of 30 s duration on an area of about 180x180μm. The 30 seconds recording were excluding initial lamp induced transients. Ultraviolet Hg lamps were used as excitation light (365 nm and 405 nm emission lines, the photoluminescence was detected through a color filter centered about 450 nm to cut away unwanted UV signal from the GaN bulk layer). Since the main purpose of the investigation is to study the blinking points time correlation, we have chosen an arbitrary reference blinking point and for each pixel intensity time-series we calculated the cross correlation to it. All our observations were made using the sole 365 nm excitation light that excites both the InGaN layer and the GaN layer[3].

Firstly, using 30 seconds PL recordings, the standard deviation was calculated for all positions and visualized as standard deviation (SD) maps to identify the location of the blinking point (that is: if the PL is constant in a location, the standard deviation should be zero, if instead it fluctuates there will be a positive SD). Then, in each sample, one blinking point is selected as the reference point to obtain the correlation coefficient with all other positions and visualized as correlation coefficient (CC) maps.

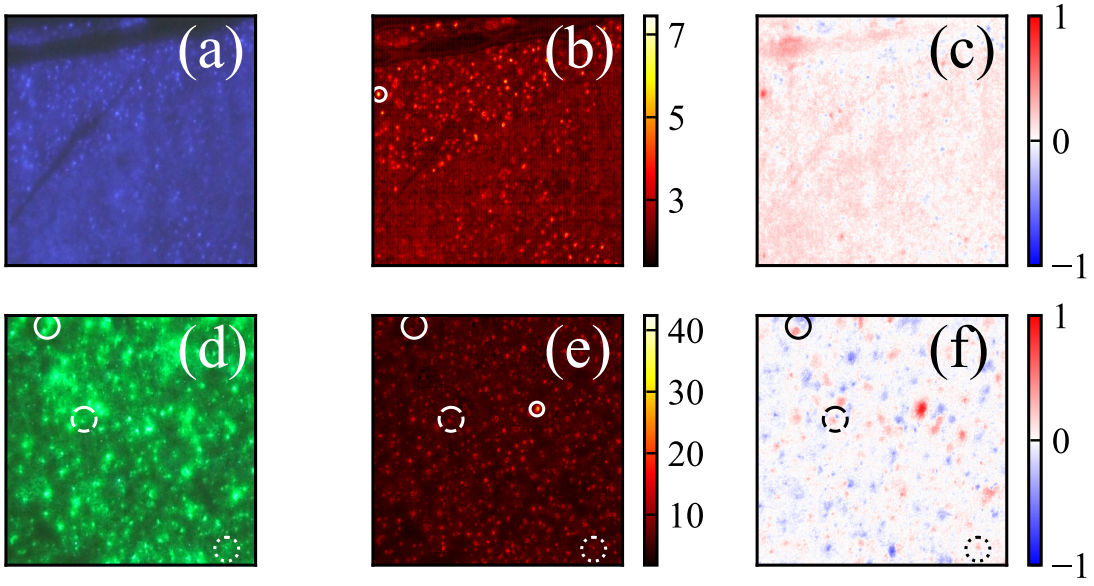

FIG. 1. The photoluminescence of the two samples (left), standard deviation maps (middle) and correlation maps (right). Top and bottom row correspond to 460 nm and 510 nm sample respectively. Each image is about 180 μ m in size and comprises of 730 pixel in both directions. The standard deviation and correlation maps are obtained elaborating the 900 points PL time-series associated for each CCD's pixels. The correlation is in respect to an arbitrary blinking point chosen as reference, indicated by the solid circle in panel (b) and (e). The maps in (c) and (f) represent the correlation coefficient of all the other pixels time-series with the reference one. The circled areas in (f) are regions where positive/negative correlation blinking domains are present.

Figure 1 shows the results of the PL measurements, its correlation analysis. The standard deviation (SD) and correlation coefficient (CC) maps were obtained from the PL measurements, using the 900 points time-series recorded for each pixels in the image. From that, we calculated the SD of the optical intensity during the 30 s recording, and plotted a value for all positions resulting in the images. In this way, we could visualize the location of the blinking points (we consider a blinking point any region where the standard deviation is bigger than 7). Let's compare the photoluminescence maps on the left and the corresponding images in the center that represent the fluctuations amplitude of those points during the 30s recording. Noticeably, all blinking points correspond to bright emission regions (ILCs), but not all ILCs do blink. Moreover, the blinking locations seen in the central image, are smaller in area than the corresponding ILCs visible in the photoluminescence maps on the left. Comparing the left and right images, we note that some

blinking domains are actually not so intense in luminescence as others. On the central panels, for each sample, one blinking point is selected as the reference to obtain the cross correlation (CC) with all positions. The CC coefficient is then visualized as color map, red for positive correlation and blue for negative on the right. As the figure shows (Fig. 1(a)), the 460 nm sample has large areas of stable luminescence and small SD (Fig. 1(b)).

Figure 1 shows these PL measurement results in panels (a) and (d), SD maps in (b) and (e), and the CC maps in (c) and (f). It can be qualitatively understood from the PL maps that there are many bright and isolated emission centers in the 510 nm sample. The SD maps show that the 460 nm sample has many areas with small SD and shows comparatively stable luminescence, while the 510 nm sample has many intense blinking points. Intriguingly, the CC maps show that the PL fluctuations are not completely random, but a residual correlation to far away regions is present. The 460 nm sample, which exhibits stable luminescence, shows that the entire sample has relatively uniform correlation in respect to a reference point circled in panel (b). The 510 nm CC map instead shows a complex structure with positive and negative correlations relative to the circled point in (e). In addition, blinking points with positive or negative correlation coefficients exist in pairs adjacent to each other. This results are congruent with previous studies[21] where samples immersed in liquids cause intense BP and show similar maps. While we found that the emission intensity changes over a broad region that has positive correlation in the 460 nm sample, we observed a spatially distant correlation in the 510 nm sample. This observation can be assumed to be important to understand the root causes of the blinking phenomenon.

The histogram in Fig. 2 shows the distribution of the correlation values of the whole image and it appears as a Gaussian distribution. To verify this relationship, a normal distribution with the same mean and standard deviation as the experimental one is plotted in Fig. 2 (red solid line). The similarity with a perfect Gaussian distribution indicates that there is almost an equal number of blinking points with opposite correlation.

Figure 3, shows PL curves of three pairs adjacent blinking points that fluctuate with opposite correlation relatively to a distance reference blinking point, the smaller circle in figure 1(e). Panel (a) shows the three pairs of curves with positive (magenta) and negative (cyan) correlation. We call them "pairs" for the simple reason that they are located at a close distance to each other. The experimental points are fitted with a fifth order polynomial curve as a guide for the eyes. These results indicate that when one of the point is increasing in intensity, the other one in the pair is decreasing. By averaging the intensities for each of those in Fig. 3(a), the curves in Fig. 3(b) are

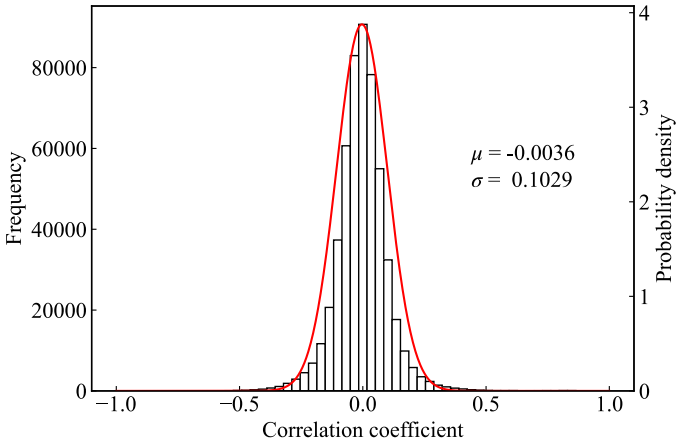

FIG. 2. Histogram for the correlation coefficients map of the 510 nm emission sample in figure 1(f). The mean and standard deviation of the distribution are reported in the inset. A red line represents the normal distribution with same mean and standard deviation of the observation.

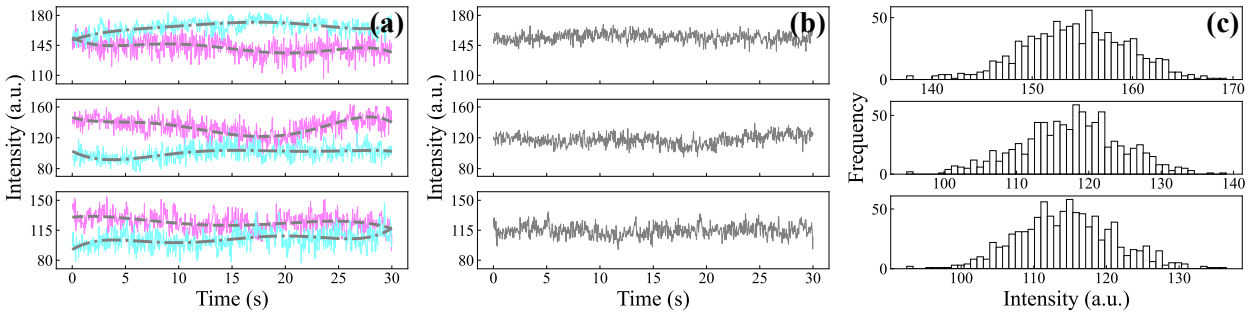

FIG. 3. (a)Intensity changes of three pairs of blinking points in the 510 nm sample of figure1(d). Magenta and cyan lines correspond to positive and negative coefficients in the correlation map respectively, also the gray dashed and dot-dashed lines are 5th order polynomial fitting of them, indicated as $I_f(t)$ in the equations in the text. The top panel represent the PL intensity profile of the pair regions in the position represented with the solid circle, the middle panel the dashed circle and the bottom panel the dotted circle. In the circles two distinct small areas with high positive (magenta) and negative (cyan) correlation are noticeable. (b)The mean of two near blinking points intensity chosen as in panel (a). In (c) is shown histograms of the averaged intensities in panel (b).

obtained. Notably, the averages are almost constant in time, suggesting that carrier recombination has a common source for each pair. Panel (c) shows the histogram of the intensities of panels (b) and all of the distributions seem to have a symmetric Normal distributed shape.

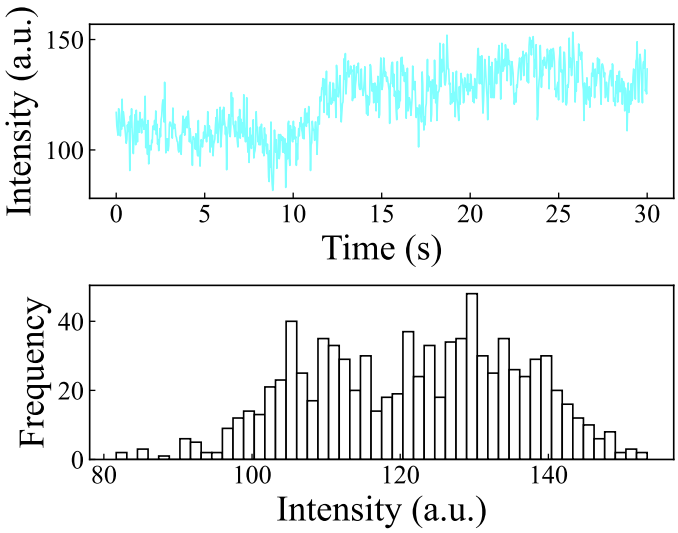

FIG. 4. An example of quasi-telegraphic (binarized) intensity blinking in our 510nm emission sample. The upper panel shows the intensity profile of one point of and the lower panel its histogram that shows two distinct peaks, characterizing the telegraphic behaviour. These points were very rare to find and are not indicated in Fig. 1.

Previous studies have reported paired blinking points[3] which can be viewed as a two-state PL emission behavior, that is the PL mainly falls on two distinct intensity levels. In our current experiment, the general behaviour was not-telegraphics, that is those kind of blinking points were very rare to find (we found only one that blinks in a fashion that could be considered as "binary") and were neglected in the theoretical analysis. As an example we show one of these fluctuations in figure 4 with its double peaked distribution.

To summarize the results obtained so far, the blinking phenomenon is often found on adjacent blinking points whose intensity changes with positive or negative correlation. Their CC, with respect to a distant reference blinking point, follows a normal distribution (Fig. 2). In addition, the averaged intensities of adjacent pairs, that have opposite correlation, is an almost constant Normally distributed profile as in figure 3(b). This fact suggests that the carrier recombination at the blinking points pairs are originated from a common nearby carrier source to that pair, with the intensity of one blinking area increasing, while that of the other is decreasing of about the same amount.

Now, we attempt to formulate a rigorous mathematical description for the BP behavior. To simplify the problem, we deal only with the intensity change of two blinking pairs. Based on

the results so far, two conditions need to be fulfilled: (a) the two blinking points have opposite correlation and (b) averaging the intensities between the two points leaves only a constant offset plus a Normally distributed residual.

Condition (b) can also be phrased as saying that if we take the average of the two functions, we are left with pure noise. As a consequence, the function that describes the intensity changes of each blinking point can be expressed as the sum of three contributions: a main form term $I_f(t)$, a noise term $I_{pn}(t), I_{nn}(t)$ and a constant offset term I_{p0}, I_{n0} (the subscript p and n represent the positive or negative correlation). Therefore, the intensity of a pair of blinking points is expressed as:

$$I_p(t) = I_f(t) + I_{pn}(t) + I_{p0}, \tag{1a}$$

$$I_n(t) = -I_f(t) + I_{nn}(t) + I_{n0}, \tag{1b}$$

These theoretical functions are representing the experimental results of Fig. 3(a). If we then take the average of Eq. (1a) and (1b), the result is expressed as:

$$\begin{aligned} I_m(t) &= \frac{I_p(t) + I_n(t)}{2} \\ &= \frac{I_{pn}(t) + I_{nn}(t) + I_{p0} + I_{n0}}{2} \\ &= I_{mn}(t) + I_{m0} \end{aligned} \tag{2}$$

Where $(I_{pn}(t) + I_{nn}(t))/2$ and $(I_{p0} + I_{n0})/2$ are replaced with $I_{mn}(t)$ and $I_{m0}(t)$ respectively. This function describes the result of Fig. 3(b), where we see a constant level of noise for all the 30 s of recording.

Now, we consider the quantum confined Stark effect taking in account the two conditions (a) and (b) mentioned above. QCSE is observed when the internal electric field generated inside a quantum well affects the charge carrier wavefunctions, therefore affecting the recombination probability and finally the photoluminescence. The electric field due to the piezoelectric properties of the material is modulating the wavefunction properties. Restricting ourselves to the phenomenological aspect, we suppose that some carriers are trapped in deep levels near the QW or that are emitted from the same traps. Thus we assume that the PL intensity is reduced if carriers are trapped and increases when instead released[16,22]. Such trapping/emission of charge carriers is considered to be stochastic and, based on the discrete nature of electric charge[23], the exchange of carriers at deep levels follows a Poisson distribution. Since there is a great number of recombination events, we can simplify this further by assuming that this Poisson distribution P can be approximated by

a normal distribution, as follows:

$$P(\mu) \approx N(\mu, \mu) \tag{3a}$$

$$P(\lambda) \approx N(\lambda, \lambda) \tag{3b}$$

Where the stochastic variable following Eq. (3a) represents the number of carriers migrating from the positive correlation region to the negative one, and (3b) represents the vice versa. Here, according to Poisson statistics, the two parameters in the brackets of the normal distribution N are identical and represent the mean and the variance respectively. Now, if we consider the number of carriers in each trap as the the difference between Eq. (3a) and Eq. (3b). Taking in account that we have two traps that have opposite correlation, using the properties of the normal distribution it follows that

$$N(\lambda - \mu, \lambda + \mu) = N(\xi, \lambda + \mu) \tag{4a}$$

$$N(\mu - \lambda, \mu + \lambda) = N(-\xi, \mu + \lambda) \tag{4b}$$

Where Eq. (4a) and Eq. (4b) are the distribution for the number of exchanged carriers in the trap for the positive and negative correlation area. The parameter ξ represents $\lambda - \mu$. If ξ is larger than 0, the recombination rate (that is the PL intensity) in positively correlated regions increases and vice-versa (if ξ is smaller than 0, this relationship is reversed). Noticeably the variance results to be $\lambda + \mu$ for both cases. For comparison with our experimental observations, finally, we examine the distribution obtained by averaging Eq. (4a) and Eq. (4b). From the properties of the normal distribution, the mean of the distributions in Eq. (4a) and Eq. (4b) is

$$N(0, \frac{\lambda + \mu}{2}) \tag{5}$$

This means that the average number of exchanged carriers trapped in the positive and negative correlation area follows a normal distribution with mean 0 and variance $(\lambda + \mu)/2$. This corresponds to the experimental results of Fig. 3(c).

We now introduce the time dependence (t) symbol and summarize the correspondence between the variables described previously and the distributions parameter of above:

$$I_f(t) \leftrightarrow \xi(t) \tag{6a}$$

$$I_{pn}(t), I_{nn}(t) \leftrightarrow N(0, \lambda(t) + \mu(t)) \tag{6b}$$

$$I_{mn}(t) \leftrightarrow N(0, \frac{\lambda(t) + \mu(t)}{2}) \tag{6c}$$

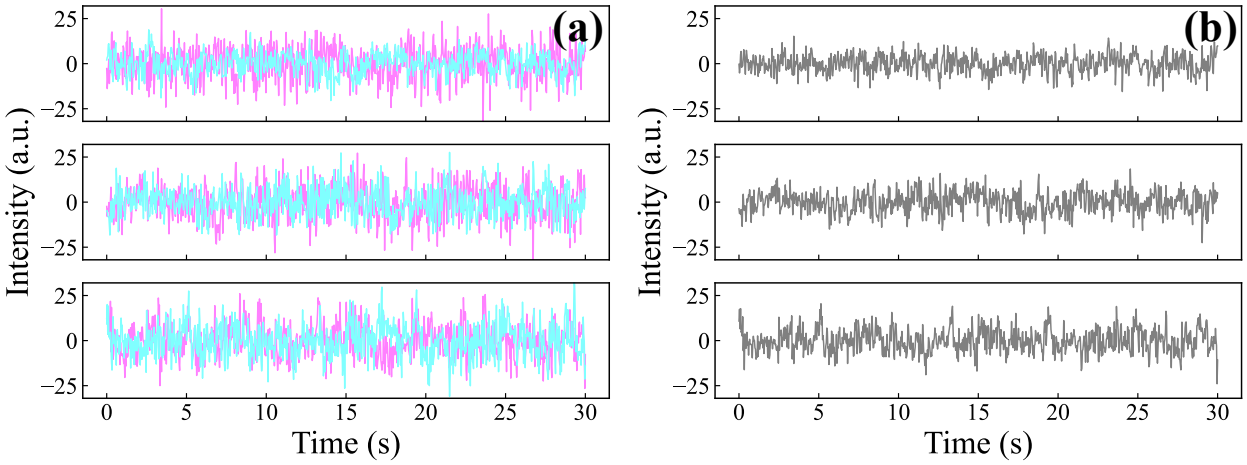

FIG. 5. (a) Residual signals obtained subtracting the PL intensities of Fig. 3(a) with the interpolation curves $I_f(t)$. (b) The average of the two intensity curves in panel (a).

In this way $I_f(t)$ represents the amount of carriers exchanged, and it corresponds to $\xi(t)$ for both the positive to negative correlation areas. This rigorously shows how the intensity fluctuations in each regions and the averaged intensity between them results to be normally distributed and associated to the amount of exchanged carriers.

Using this formalism, the dotted curves in Fig. 3(a) are both represented by the same function $\xi(t)$ for each pair of blinking points. Subtracting it to the photoluminescence we obtain the I_{pn} and I_{nn}. This is evident from the experimental data plotted in Fig. 5(a).

Now, in the same fashion, when we take the average intensities of the experiments in Fig. 5(a) and obtain Fig. 5(b). Our formalism predicts that the variance of this should be half that of the two PL intensities before the averaging (see Eq. (5)).

To confirm the above, we have chosen ten pairs of negative/positive correlation regions. These are ten blinking areas chosen using from figure 1(f), each of them include pairs of blinking points of opposite correlation as in Fig. 3(a). We examined their variance, before and after averaging the pairs, and plotted the SD value. The result is shown in Fig. 6. The box on the left panel, indicated symbolically on the horizontal axis with I_{pn}, I_{nn}, is the variance calculated over the twenty individual positive or negative correlation regions. The other box on the right, symbolized on the horizontal axis as I_{mn}, represents instead the ten variance values obtained by averaging each positive/negative pairs. We point out that the variance is obtained from 30 s recordings, these

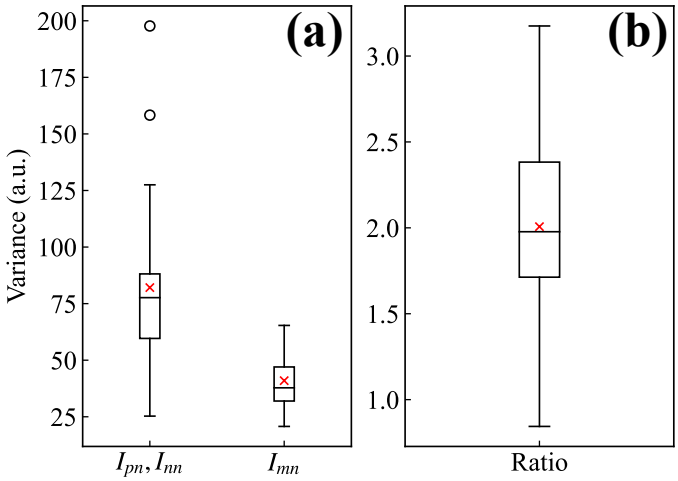

FIG. 6. Box plots for the variance of intensities (left) and for their ratios (right). The red crosses indicate averages. The labels on the horizontal represent the experimental data for the positive correlation and the negative correlation areas (I_{pn}, I_{nn}), and the average of them I_{mn}. The I_{pn}, I_{nn} box comprises of 20 variance values, the box on the right (I_{mn}) comprises of 10 variance values, obtained after averaging the PL time-series of the adjacent blinking pairs with positive and negative correlation. The fact that the averages of these two class of variances has a relation of about 2:1, panel (b), as predicted in Eq. 6c is not trivial.

intensity values should be completely independent from each other. On the contrary, we found that their variances are related as Eq. (5). This shows that the variance of the intensity, centered around the value 2, is about half the value before averaging. This is consistent with what is theoretically predicted.

Two different ways of understanding BP, experimental formulation and model with statistics, lead to equal result and support the validity of our hypothesis. Since this hypothesis is consistent with the application of QCSE to explain the optical memory effect in InGaN thin films[16], this is the first step toward providing a unified theoretical background for complex optical phenomena in InGaN-based materials, as well as in InGaN single QW.

We thank Yokohama City University for the its support with the "Research Fund 2022" that helped the realization of this research.

Experimental data are available upon reasonable request.

REFERENCES

[1]S. Strite and H. Morkoç, "Gan, aln, and inn: A review," Journal of Vacuum Science and Technology, B **10**, 1237–1266 (1992).

[2]F. Stefani, J. Hoogenboom, and E. Barkai, "Beyond quantum jumps: Blinking nanoscale light emitters," Phys. Today **62**, 34–39 (2009).

[3]R. Micheletto, M. Abiko, A. Kaneta, Y. Kawakami, Y. Narukawa, and T. Mukai, "Observation of optical instabilities in the photoluminescence of ingan single quantum well." Applied Physics Letters **88**, 061118 (2006).

[4]A. Kaneta, M. Funato, and Y. Kawakami, "Nanoscopic recombination processes in ingan/gan quantum wells emitting violet, blue, and green spectra," Phys. Rev. B **78**, 125317 (2008).

[5]R. Micheletto, N. Yoshimatsu, A. Kaneta, Y. Kawakami, and S. Fujita, "Indium concentration on pl spatial in homogeneity in ingan single quantum well structures detected by an original low cost near-field probes," Applied Surface Science **229**, 338–345 (2004).

[6]Y. Narukawa and Y. Kawakami, "Role of self-formed ingan quantum dots for exciton localization in the purple laser diode..." Applied Physics Letters **70**, 981 (1997).

[7]S. Chichibu, T. Azuhata, T. Sota, and S. Nakamura, "Spontaneous emission of localized excitons in ingan single and multiquantum well structures." Applied Physics Letters **69**, 4188 – 4190 (1996).

[8]R. Micheletto, M. Allegrini, and Y. Kawakami, "Near-field evidence of local polarized emission centers in ingan/gan materials," Applied Physics Letter **95**, 211904 (2009).

[9]M. Nirmal, B. O. Dabbousi, M. G. Bawendi, J. J. Macklin, J. K. Trautman, T. D. Harris, and L. E. Brus, "Fluorescence intermittency in single cadmium selenide nanocrystals," Nature **383**, 802–804 (1996).

[10]D. Bertram, M. Hanna, and A. Nozik, "Two color blinking of single strain-induced gaas quantum dots," Applied Physics Letters **74**, 2666–2668 (1999).

[11]A. Efros and M. Rosen, "Random telegraph signal in the photoluminescence intensity of a single quantum dot," Physical Review Letters **78**, 1110–1113 (1997).

[12]R. Cook and H. Kimble, "Possibility of direct observation of quantum jumps," Physical Review Letters **54**, 1023–1026 (1985).

[13]M. Sugisaki, H.-W. Ren, S. V. Nair, K. Nishi, and Y. Masumoto, "External-field effects on the optical spectra of self-assembled inp quantum dots," Phys. Rev. B **66**, 235309 (2002).

[14]Y. Kawakami, A. Kaneta, K. Omae, A. Shikanai, K. Okamoto, G. Marutsuki, Y. Narukawa, T. Mukai, and S. Fujita, "Recombination dynamics in low-dimensional nitride semiconductors," physica status solidi (b) **240**, 337–343 (2003).

[15]T. Takeuchi, S. Sota, M. Katsuragawa, M. Komori, H. Takeuchi, H. Amano, and I. Akasaki, "Quantum-confined stark effect due to piezoelectric fields in gainn strained quantum wells," Jpn. J. Appl. Phys. **36**, L382 (1997).

[16]B. B. Wang, J. J. Zhu, D. G. Zhao, D. S. Jiang, P. Chen, Z. S. Liu, J. Yang, W. Liu, F. Liang, S. T. Liu, Y. Xing, L. Q. Zhang, and M. Li, "Deep levels induced optical memory effect in thin ingan film," AIP Advances **8**, 085222 (2018).

[17]J. Speck and S. Rosner, "The role of threading dislocations in the physical properties of gan and its alloys," Physica B: Condensed Matter **273-274**, 24–32 (1999).

[18]A. Y. Polyakov and I.-H. Lee, "Deep traps in gan-based structures as affecting the performance of gan devices," Materials Science and Engineering: R: Reports **94**, 1–56 (2015).

[19]R. Micheletto, K. Oikawa, and C. Feldmeier, "Observation of lattice thermal waves interference by photoluminescence blinking of ingan quantum well devices," Applied Physics Letters **103**, 17109 (2013).

[20]T. Tsutsumi, G. Alfieri, Y. Kawakami, and R. Micheletto, "The relation between photoluminescence properties and gas pressure with 0001 ingan single quantum well systems," Applied Surface Science **392**, 256–259 (2017).

[21]S. Yoshida, Y. Fujii, G. Alfieri, and R. Micheletto, Semicond. Sci. Technol. **37**, 095009 (2022).

[22]C. Feldmeier, M. Abiko, U. T. Schwarz, Y. Kawakami, and R. Micheletto, "Transient memory effect in the photoluminescence of ingan single quantum wells," Opt. Express **17**, 22855–22860 (2009).

[23]Y. Blanter and M. Büttiker, "Shot noise in mesoscopic conductors," Physics Reports **336**, 1–166 (2000).